Polímeros
ISSN 1678-5169 (Online)

https://doi.org/10.1590/0104-1428.20240034

ORIGINAL ARTICLES

Thermal and mechanical properties of filaments for additive manufacturing[a]

Iago Rodrigues de Abreu[1], Renato de Sousa Nascimento Junior[1], Allef Gabriel Da Silva Fortes[1], Rudy Folkersma[2], Luigi Veloso Leitão[3], Fabio Delano Penha Marques[3], Arthur Antônio Sousa Sampaio[3], Layara Lorrana Ribeiro Leite de Castro[1], Daniella Stepheny Carvalho Andrade[4], Tatianny Soares Alves[1,3] and Renata Barbosa[1,3]*

[1]Laboratório de Polímeros e Materiais Conjugados – LAPCON, Programa de Pós-graduação em Ciência e Engenharia dos Materiais - PPGCM, Universidade Federal do Piauí – UFPI, Teresina, PI, Brasil
[2]NHL Stenden University of Applied Sciences, Emmen, Netherlands
[3]Curso de Engenharia de Materiais – CT, Universidade Federal do Piauí – UFPI, Teresina, PI, Brasil
[4]Curso de Engenharia de Materiais – CT, Universidade Federal de Pernambuco – UFPE, Recife, PE, Brasil
**rrenatabarbosa@yahoo.com*
[a]**This paper has been partially presented at the 17th Brazilian Polymer Congress, held in Joinville, SC, 29/Oct - 02/Nov/2023**

Abstract

This study explores the development of biodegradable filaments for additive manufacturing, aiming to create membranes for oil and water separation. Using a mixture of poly (lactic acid) and poly (butylene adipate co-terephthalate) (PLA/PBAT) with additives such as zinc oxide, biocide and carnauba wax. The research evaluates the potential of these materials in membrane prototyping for this application. Characterization techniques such as FTIR, XRD, DSC and tensile strength were employed. The results showed that the addition of the additives did not induce the formation of new bands in the FTIR. However, new diffraction peaks appeared in the composites indicating the presence of the zinc oxide. DSC revealed a double peak in melting and crystallization temperatures and the mechanical tests showed significant influence of additives on tensile strength. The composite filaments proved to be suitable for 3D printing, suggesting their applicability in the manufacture of filter membranes for oil and water separation.

Keywords: *additive manufacturing, material extrusion, zinc oxide, biocide, carnauba wax.*

How to cite: Abreu, I. R., Nascimento Junior, R. S., Fortes, A. G. D. S., Folkersma, R., Leitão, L. V., Marques, F. D. P., Sampaio, A. A. S., Castro, L. L. R. L., Andrade, D. S. C., Alves, T. S., & Barbosa, R. (2024). Thermal and mechanical properties of filaments for additive manufacturing. *Polímeros: Ciência e Tecnologia*, *34*(3), e20240025. https://doi.org/10.1590/0104-1428.20240034

1. Introduction

The distribution and supply of drinking water is indispensable in society, but the ongoing contamination of aquatic environments remains a constant challenge and a significant environmental problem that requires efficient solutions. Sources of pollution arise from various sectors, including agriculture, steel production, textiles, food and petrochemical industries, responsible for the emission of a range of pollutants, from water-soluble toxic compounds to insoluble oily substances[1,2]. Several technologies have been used in the industrial sphere to treat and/or mitigate the effects of this pollution. Processes including centrifugation, chemical coagulation, membrane filtration, physical adsorption, and ionic filtration are often criticized for their high operating costs and the generation of additional waste that can harm the environment[3-5].

Recently, the adoption of microfiltration membranes has emerged as an effective solution, both as a primary treatment and as a complement to conventional purification methods, especially those that have specific wettability properties. They are mainly used due to characteristics such as efficiency, low energy consumption and structure[6]. However, challenges such as membrane sizing caused by particle aggregation represent a point and a gap to be addressed in research and development aimed at improvements[7].

Among the manufacturing technologies currently available, additive production, commonly known as 3D printing, emerges as a notable innovation, offering the ability to produce complex parts at reduced costs. This technology is particularly valued for its versatility and design freedom, allowing the development of functional devices with different architectures[8,9]

The literature reports the manufacture of materials with superhydrophilic and superoleophobic characteristics by 3D printing for oil/water separation, mainly with surface

functionalization. Li et al.[10] produced special superhydrophilic and superhydrophobic membranes by 3D inkjet printing (Binder Jetting) using cellulose acetate, polyvinyl alcohol and silica nanoparticles, achieving high efficiency in oil/water separation.

Furthermore, nanostructured materials have currently received attention in wastewater treatment we can mention some materials such as: Zeolite Minerals[11], Biochar[12], graphene oxide – GO[13,14], titanium dioxide - TiO_2[13,15,16], iron oxide – FeO[17]and zinc oxide – ZnO[9].

Oil-water separation techniques face several technical challenges, from pore size specificity to membrane surface characteristics such as roughness and ability to repel or attract water (wetting). One of the main problems encountered is the clogging of the membrane pores by oil incrustation, significantly reducing filtration efficiency. To overcome these obstacles, solutions such as antifouling coatings stand out; they often combine biocides with other compounds to prevent oil accumulation in membranes[18-20].

Natural materials emerge in this field of research mainly due to their physical-chemical properties, cost-benefit and positive environmental impact, offering sustainable alternatives for water treatment[21,22]. For example, carnauba wax, obtained from the leaves of the Copernicia prunifera palm, is notable for its applications on self-cleaning and antifouling surfaces, as well as possessing anti-fog and anti-corrosion Properties[23,24]. In addition, the incorporation of biocidal agents provides an effective solution to the challenge of microbial fouling, a common problem in industrial and aquatic environments. In this way, these materials are able to prevent the adhesion and growth of harmful organisms on their surfaces, particularly valuable in pipelines and water purification systems to maintain operational efficiency and safety[25].

In addition to this, the adoption of biodegradable materials, such as the Ecovio® blend, composed of polylactic acid (PLA) and (PBAT), represents an environmentally responsible strategy. These materials have been used in the production of filters with antimicrobial properties, highlighting the commitment to sustainability in water treatment[26].

Based on the above, the objective of this study was to produce biodegradable polymeric filaments by extrusion, intended for use in additive manufacturing processes that employ the filament extrusion technique for prototyping filter membranes with specific wettability properties, intended to optimize oil separation treatment. and water.

2. Materials and methods

2.1 Materials

The commercial blend Ecovio® (EC), produced by BASF SA, and formed by Poly (lactic acid) - PLA and Poly (butylene adipate-co-terephthalate) - PBAT, was used as the polymeric matrix. The following additives were used to form the composites: Sanitized Commercial Biocide MB E 22-70 (BCD), Zinc Oxide (ZnO) and Carnauba Wax (CW).

2.2 Preparation of the composites and filaments

The materials were previously mixed using concentrations of 3 e 5% for zinc oxide and 1% for the biocide and carnauba wax, respectively, in relation to the polymeric blend. Subsequently, the compositions were processed in a single-screw extruder model AX-16 from AX plastics (L/D = 26) under a temperature profile of 170, 175 and 180 °C and screw speed of 40 rpm. The composite obtained was cooled in water and granulated in a pelletizer.

The pelletized composites obtained were dried in an oven at 80 °C for 4h and soon after the filaments were prepared using the same single screw extruder under the same processing conditions. The cooling was carried out by bathing in water and aid of a chillers of the brand Filmaq3D. The dimensions of the filaments were controlled by means of a reel, of the same brand, acting in the process of pulling the filaments, allowing adjustment of diameter of 1.75 ± 0.10 mm during the process.

2.3 Characterizations

2.3.1 Fourier transform infrared spectroscopy - FTIR

FTIR spectra were obtained on a Nicolet Summit FTIR spectrometer operating in attenuated total reflectance (ATR) mode. The scan was used in the range of 4000 to 500 cm^{-1}, totaling 16 scans in the analysis. The analyzes were carried out in the GREENPAC laboratory (Polymer Application Center - NHL Stenden), Netherlands.

2.3.2 X-ray Diffraction - XRD of Composite Filaments

The filaments were evaluated in a Bruker X-ray diffractometer, model D6 phaser. The incident radiation used was the Cu-Kα (λ = 1.5406 Å) scan between 5 and 75° (2θ), at a speed of 2/min at a power of 40 kV/30mA. The analysis was conducted at the University of Groningen (Groningen - Netherlands) in the Department of Macromolecular Chemistry & New Polymer Materials.

2.3.3 Differential Scanning Calorimetry - DSC

The DSC analysis of the filaments was carried out using a TA Instruments® DSC25 under a nitrogen atmosphere, in aluminum crucibles, and a heating ramp of 10°C/min with a scanning range between -20 and 200°C. The analyzes were carried out at the Green PAC – Polymer Application Center located at the NHL Stenden University of Applied Sciences (Emmen – Netherlands).

2.3.4 Tensile strength

Tensile strength testing was performed on the filaments in accordance with ASTM D3379. Five samples of each composition were selected, and the test was carried out at a speed of 5 mm/min, with a 5 kN load cell on an EMIC universal machine, model DL 30000, belonging to the Materials Engineering Course at the Federal University of Piauí.

2.3.5 Statistical Analysis

The data obtained from the tests tensile strength were statistically analyzed. For this, we used the analysis of variance (ANOVA) through the OriginPro software. Additionally, the Tukey test was applied to identify significant differences between the data sets, adopting a significance level of 5%. This methodology allowed to verify relevant changes with $p > 0.05$.

3. Results and Discussions

3.1 Fourier Transform Infrared Spectroscopy - FTIR of composite filaments

The FTIR spectra of the composite filaments (EC/3ZnO; EC/5ZnO; EC/3ZnO/BCD; EC/5ZnO/BCD; EC/3ZnO/BCD/CW and EC/5ZnO/BCD/CW) and the polymer matrix (EC) are presented in Figure 1.

The FTIR spectra of the pure mixture (EC) filaments showed characteristic bands of the two polymers that compose it. Thus, bands can be observed in the region of 2923 cm^{-1} and 2849 cm^{-1} associated with symmetric and asymmetric stretching vibrations of the CH_2 and CH_3 groups[27,28]. Bands at 1712 cm^{-1} and 1754 cm^{-1} referring to the C=O stretching vibrations (ester group) present in PLA and PBAT[28,29]. The bands observed at 1455 cm^{-1} and 1270 cm^{-1} refer, respectively, to the asymmetric bending vibration of the CH_3 group of the PLA phase and the symmetric stretching vibration of the CO of the PBAT phase[30,31]. At 1180 and 1080 cm^{-1}, the bands are characteristic of C=O stretching vibration[29]. The bands at 872 and 757 cm^{-1} are attributed to the absorption of the ester group and the vibration absorption of the α-methyl group, in addition, they can also be attributed to the amorphous and crystalline phases of PLA, respectively (Malinowski et al., 2020)[32]. The bending vibration band of the CH plane of the benzene ring of PBAT is represented at 728 cm^{-1}[29,30]. It was not possible to observe modification or emergence of new absorption bands with the incorporation of additives.

In relation to zinc oxide, the main filler in the composite, it was also not possible to identify the formation of new bands due to the insertion of this filler. The literature reports Zn-O stretching in the regions of 906 - 644 cm^{-1} and 1507 - 1378 cm^{-1} attributed to the asymmetric stretching of the oxygen present in the composition[33,34]. The insertion of ZnO may have caused greater degradation of the PBAT phase as reported in the literature in bands that are identified by the absorption of carboxylic groups or carboxylates at 1660, 1550, 1424 and 969 cm^{-1} [35].

The literature reports bands related to the bonds CH, C=O, C≡C, CN, NH at 1848, 1468, 1515, 1161 and 722 cm^{-1}, respectively, in carnauba wax[36]. Likewise, the biocidal compound encapsulated with EVA did not induce changes in the composites, possibly this behavior refers to the chemical groups being from the same region as the Blend, with characteristic peaks at 1736, 1370, 1238, 1020 and 608 cm^{-1} [37]. From this discussion, the absence of new bands in the composites compared to the polymeric blend indicates that there was no interaction with the incorporation of additives.

3.2 X-ray Diffraction - XRD of composite filaments

Figure 2 shows the diffractograms of the composite filaments. The XRD curves for the blend filaments showed peaks related to the phases that make up the blend. Due to the semi-crystalline profile of the polymer, it is possible to observe a large amorphous halo and some well-defined peaks. Peaks were detected at 15.6°, 17.4°, 20.4°, 23° and 24.8° referring to the PBAT phase, respectively, corresponding to the planes (010), (111), (100) and (111)[38,39].

The crystalline phase of PLA is observed in peaks close to those found in the PBAT phase. The literature reports peaks

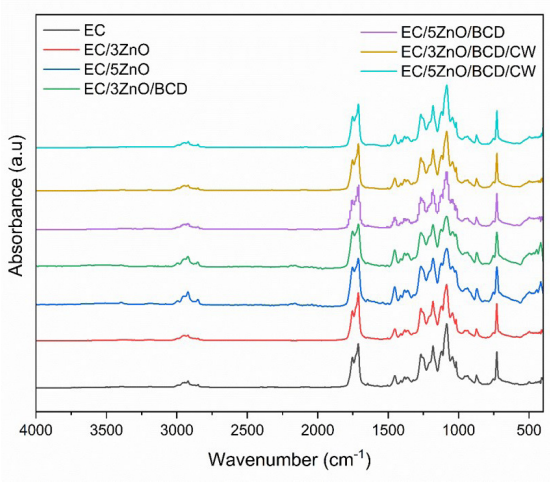

Figure 1. Infrared spectrum for the compositions EC, EC/3ZnO, EC/5ZnO, EC/3ZnO/BCD, EC/5ZnO/BCD, EC/3ZnO/BCD/CW and EC/5ZnO/BCD/CW

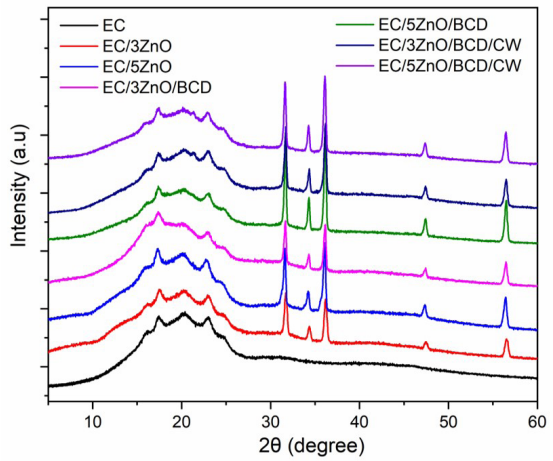

Figure 2. Diffractography of filaments EC, EC/3ZnO, EC/5ZnO, EC/3ZnO/BCD, EC/5ZnO/BCD, EC/3ZnO/BCD/CW and EC/5ZnO/BCD/CW

2θ = 16.76° and 19.26° referring to the crystallographic planes (200) and (201)[40,41].

For zinc oxide, the main diffraction peaks were found at 2θ of 31.8°, 34.5°, 36.3°, 47.6°, 56.6°, 62.9° and 68° characteristic of this compound, with these peaks referring to planes (100), (002), (101), (102), (110), (103) and (112), respectively, corroborating the card (JCPDS 36-1451) and literature[42-45]. Carnauba wax has a semi-crystalline characteristic that can be visualized, with main peaks of greater intensity observed at angles of approximately 21.5°, 24.1°, as also reported by[46-49]. As previously mentioned, the biocide is a compound formed by zinc pyrithione loaded into EVA that presents characteristic peaks in at 21.9° and 23.8° referring to the orthorhombic system of the EVA unit cell, respectively for o plans (110) and (200)[45,50]. Possibly the pyrithione peaks were overlapped by the EVA peaks or it was not possible to read them, the literature reports two diffraction peaks at 11.1° and 22.5° for this compound[51].

3.3 Differential Scanning Calorimetry - DSC of composite filaments

The thermal behavior by determination of glass transition temperature (Tg), cold crystallization temperature (Tcc) and crystalline melting temperature (Tm) is presented in Figure 3. The main function of the first heating is to quench the heat history in the material, but it can be of fundamental importance in the study of the aging of the material[52]

The curves indicated that the glass transition temperatures in all filaments showed values close to 65 °C in both the first and second heating. The literature reports that such thermal event is related to the PLA phase present in the blend. The insertion of additives in the PLA/PBAT matrix did not imply the change of this thermal transition[52-55].

It is also possible to observe an exothermic event after the glass transition temperature of the PLA, at approximately 102 C, and prior to the crystalline melting temperature. This behavior may be related to the crystalline melting temperature (Tm) of PBAT as reported in the literature and thermal relaxation and cold crystallization of PLA molecules, because the increase in temperature implies the increase of energy in the polymer chains between the amorphous and crystalline domains[53].

For the blend curve and compositions with 3 and 5% ZnO, it was possible to observe that the crystalline melting temperature showed the same behavior. However, two crystalline fusion peaks were formed with the insertion of 1% in biocide and 1% in carnauba wax, even in lower percentage. The same behavior was recorded in the cooling stage, where the biocide and carnauba wax acted as nucleating agents in the recrystallization of the material[54,56]. This fact can be observed by the variation in the crystallinity percentage of the PLA phase with the incorporation of these additives.

The 2nd heating curves (b) showed the same behavior of the curves for the first heating, however, unlike the first ramp, only a fusion peak was detected for the compositions containing 1% of biocide and 1% of wax. Through the cooling (c) it was possible to observe that the nucleant effect of the biocide and the wax, resulted in the reduction of the crystalline melting temperature in approximately 3 °C.

Pascual-González et al.[57] produced PLA filaments with zinc oxide and observed the formation of a double crystalline melting peak and a reduction in the crystalline melting temperature for compositions with values above 7.5% of said additive.

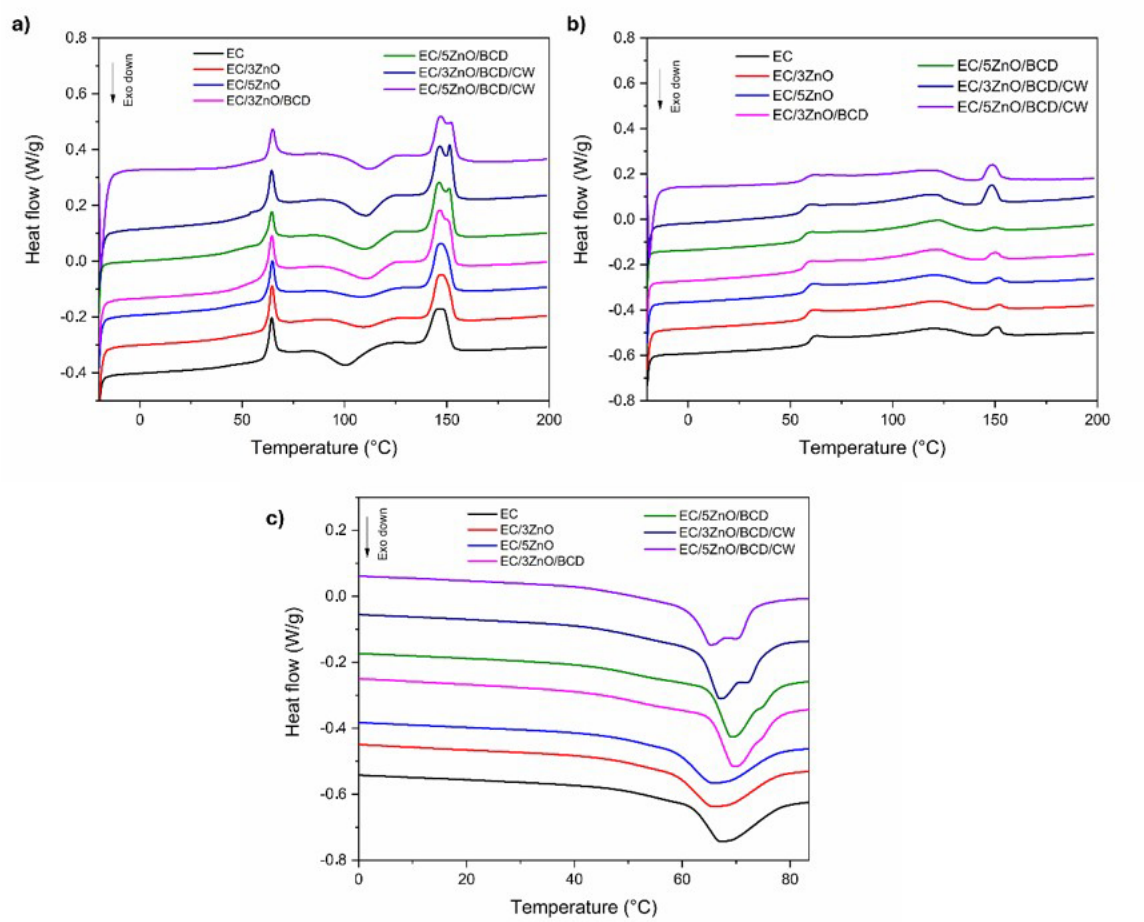

Figure 3. DSC curves for the first heating (a), second heating (b) and cooling (c) for the compositions EC, EC/3ZnO, EC/5ZnO, EC/3ZnO/BCD, EC/5ZnO/BCD, EC/3ZnO/BCD/CW, and EC/5ZnO/BCD/CW.

Increased melting and crystallization temperatures facilitate consistent solidification in the extrusion printing process, resulting in better interlayer adhesion and preventing delamination during printing. However, the DSC curves obtained during the first heating suggest that a secondary crystallization process may occur after printing, due to the additional time available for accommodation and ordering of polymer chains and the polycrystalline character with the insertion of these nucleant agents, such as carnauba wax[56]. The results presented, especially in compositions with carnauba wax, suggest a controlled crystallinity for the 3D printing process, being beneficial in reducing defects such as warping, resulting from high residual stresses, indicating a good printability.

3.4 Mechanical properties of filaments

The ability of filaments to resist tensile strength is crucial for their processability in the extrusion process. It is essential that the filament has adequate resistance to preserve its integrity during transport to the extruder as well as at the time of transport by pulleys[58]. Table 1 illustrates the mechanical behavior in terms of maximum tension and elastic modulus of filaments derived from the blend and its composites.

It was observed that the EC composition presented a higher Maximum Stress value (31.50 MPa), while the EC/3ZnO/BCD/CW sample presented a higher Elasticity Modulus (916.47 MPa). Furthermore, the behavior when tensioned presented a completely different profile for each composition. According to the results, the pure polymer filament composition generally presented the highest values of mechanical properties among the other compositions. The results indicated a slight decrease in values that can be attributed to poor filler dispersion in the filament extrusion process, resulting in poor interfacial adhesion of the additive particles with the polymer matrix[33,58].

It was also observed that when comparing the values of the modulus of elasticity of the filament blended with the EC/3ZnO composition, a reduction in the stiffness of the material was noted, however, with the incorporation of the biocide and mainly carnauba wax, the values increased to be higher than those reported in previous compositions. In this sense, the incorporation of the biocide and carnauba wax increased the rigidity of the filament. Mathew et al. [29] evaluated the tensile strength properties of filaments composed of the PLA/PBAT blend in different quantities and observed a reduction in tensile strength, flexion and modulus of elasticity with an increase in the percentage of PBAT, however, at 40% a reduction in elongation was noted due to the increase in the dispersed phase. The modulus of elasticity showed an increase in its values in relation to the little variation detected in the tensile strength. It is important to highlight that filaments produced in the laboratory on a small scale are subject to having their properties affected by factors such as humidity, variation in diameter, as well as low homogeneity in composition[59].

The results of the statistical analysis revealed that the incorporation of loads does not have significant effect when the filament is evaluated in relation to maximum strength. For the modulus of elasticity, there was a significant increase in the compositions EC/3ZnO/BCD, EC/5ZnO/BCD, EC/3ZnO/BCD/CW, EC/3ZnO/BCD/CW demonstrating greater tension in the composite, impacting the tensile strength of the filaments. This increase in stiffness is beneficial in the transport of the filament by the pulleys since the polymeric blend (EC) is a more plastic material due to the percentage of PBAT in the composition.

Table 1. Tensile strength and modulus of elasticity for the compositions EC, EC-3ZnO, EC/5ZnO, EC/3ZnO/BC, EC/5ZnO/BCD, EC/3ZnO/BC/CW and EC/5ZnO/BCD/CW.

Compositions	Tensile strength (MPa)	Modulus of elasticity (MPa)
EC	31.5 ± 1.69 ^{a}	779.19 ± 35.78 ^{b}
EC/3ZnO	26.10 ± 1.20 ^{a,d}	719.64 ± 42.65 ^{b}
EC/5ZnO	27.35 ± 1.21 ^{a,c}	793.55 ± 67.88 ^{a,b}
EC/3ZnO/BCD	26.49 ± 0.69 ^{a,b,c}	824.08 ± 37.75 ^{a}
EC/5ZnO/BCD	25.76 ± 0.63 ^{a,b,c,d}	851.96 ± 55.043 ^{a}
EC/3ZnO/BCD/CW	27.72 ± 0.58 ^{a,b}	916.47 ± 54.49 ^{a}
EC/5ZnO/BCD/CW	26.90 ± 0.66 ^{b,c,d}	756.51 ± 121.32 ^{a,b}

^{a,b,c,d} Results of groups marked with the same letter show no statistical difference ($p>0.05$) between the means according to the Tukey test.

4. Conclusions

Polymeric filaments for additive manufacturing by filament extrusion were successfully produced and had their chemical, thermal and mechanical properties evaluated. The FTIR spectra indicated the absence of new bands with the insertion of the biocide and carnauba wax into the polymeric blend, showing no chemical changes in the composites. Regarding the XRD analysis, peaks relating to the ECOVIO, ZnO, wax phase were recorded and the peaks corresponding to the biocide phase may have been overlapped by the amorphous region of the blank. DSC analysis showed double peak formation of Tm and Tcc during the first heating and cooling for compositions containing biocide and carnauba wax, as well as changes in Tm values on the second heating. The evaluation of the tensile strength properties indicated that the incorporation of additives modified the mechanical resistance. The composition EC/3ZnO/BCD/CW exhibited higher modulus of elasticity resulting in greater stiffness justified by the insertion of the biocide and wax. The filaments produced showed satisfactory properties, enabling their application as functionalized membranes in water/oil treatment. Furthermore, more studies and characterizations on the viability of the product will be necessary. Thus, with the innovative nature of the work, new perspectives are opened for the production of membranes without the need for extra surface treatment.

5. Author's Contribution

- **Conceptualization –** Iago Rodrigues de Abreu.
- **Data curation –** Iago Rodrigues de Abreu.
- **Formal analysis –** Iago Rodrigues de Abreu; Fabio Delano Penha Marques; Arthur Antônio Sousa Sampaio.
- **Funding acquisition –** Renata Barbosa; Tatianny Soares Alves; Rudy Folkersma.
- **Investigation –** Iago Rodrigues de Abreu.

- **Methodology –** Iago Rodrigues de Abreu; Fabio Delano Penha Marques; Arthur Antônio Sousa Sampaio; Luigi Veloso Leitão; Renato de Sousa Nascimento Junior; Allef Gabriel da Silva Fortes.
- **Project administration –** Iago Rodrigues de Abreu; Renata Barbosa.
- **Resources –** Renata Barbosa.
- **Software –** NA.
- **Supervision –** Renata Barbosa; Rudy Folkersma.
- **Validation –** Renato de Sousa Nascimento Junior; Luigi Veloso Leitão; Fabio Delano Penha Marques; Arthur Antônio Sousa Sampaio; Allef Gabriel da Silva Fortes.
- **Visualization –** Layara Lorrana Ribeiro Leite de Castro; Daniella Stepheny Carvalho Andrade.
- **Writing – original draft –** Iago Rodrigues de Abreu
- **Writing – review and editing –** Iago Rodrigues de Abreu; Renata Barbosa.

6. Acknowledgements

The authors would like to thank the Federal University of Piauí; the Laboratory of Polymers and Conjugated Materials (LAPCON); NHL Stenden University of Applied Sciences; GREENPAC Laboratory (Polymer Application Center); Piauí State Research Support Foundation (FAPEPI); National Council for Scientific and Technological Development (CNPq) and Funding: This work was supported by CNPq [process number: 308446/2018-6] and [process number: 308309/2022-7].

7. References

1. Luo, X., He, Z., Gong, H., & He, L. (2022). Recent advances in oil-water separation materials with special wettability modified by graphene and its derivatives: a review. *Chemical Engineering and Processing*, *170*, 108678. http://doi.org/10.1016/j.cep.2021.108678.
2. Abu-Thabit, N. Y., Uwaezuoke, O. J., & Abu Elella, M. H. (2022). Superhydrophobic nanohybrid sponges for separation of oil/ water mixtures. *Chemosphere*, *294*, 133644. http://doi.org/10.1016/j.chemosphere.2022.133644. PMid:35065181.
3. Zhu, Y., Liu, Y., Mohamed, H. F., Zheng, X., He, J., & Lin, L. (2022). Rigid, eco-friendly and superhydrophobic SiO2-Polyvinyl alcohol composite sponge for durable oil remediation. *Chemosphere*, *307*(Pt 4), 135990. http://doi.org/10.1016/j.chemosphere.2022.135990. PMid:35977562.
4. Malczewska, B., Farnood, R. R., & Tabe, S. (2022). Natural organic matter removal by electrospun nanofiber membranes coated with heated aluminum oxide particles. *Journal of Water Process Engineering*, *45*, 102498. http://doi.org/10.1016/j.jwpe.2021.102498.
5. Dias, R., Daam, M. A., Diniz, M., & Maurício, R. (2023). Drinking water treatment residuals, a low-cost and environmentally friendly adsorbent for the removal of hormones - a review. *Journal of Water Process Engineering*, *56*, 104322. http://doi.org/10.1016/j.jwpe.2023.104322.
6. Rao, L., You, X., Chen, B., Shen, L., Xu, Y., Zhang, M., Hong, H., Li, R., & Lin, H. (2022). A novel composite membrane for simultaneous separation and catalytic degradation of oil/water emulsion with high performance. *Chemosphere*, *288*(Pt 1), 132490. http://doi.org/10.1016/j.chemosphere.2021.132490. PMid:34624347.
7. Liu, L., Xiao, Z., Liu, Y., Li, X., Yin, H., Volkov, A., & He, T. (2021). Understanding the fouling/scaling resistance of superhydrophobic/omniphobic membranes in membrane distillation. *Desalination*, *499*, 114864. http://doi.org/10.1016/j.desal.2020.114864.
8. Yan, C., Ma, S., Ji, Z., Guo, Y., Liu, Z., Zhang, X., & Wang, X. (2019). 3D printing of an oil/water mixture separator with in situ demulsification and separation. *Polymers*, *11*(5), 774. http://doi.org/10.3390/polym11050774. PMid:31052425.
9. Kumbhakar, P., Ambekar, R. S., Mahapatra, P. L., & Tiwary, C. S. (2021). Quantifying instant water cleaning efficiency using zinc oxide decorated complex 3D printed porous architectures. *Journal of Hazardous Materials*, *418*, 126383. http://doi.org/10.1016/j.jhazmat.2021.126383. PMid:34329007.
10. Li, X., Shan, H., Zhang, W., & Li, B. (2020). 3D printed robust superhydrophilic and underwater superoleophobic composite membrane for high efficient oil/water separation. *Separation and Purification Technology*, *237*, 116324. http://doi.org/10.1016/j.seppur.2019.116324.
11. Kennedy, A. J., Ballentine, M. L., Das, A., Griggs, C. S., Klaus, K., & Bortner, M. J. (2021). Additive manufacturing for contaminants: ammonia removal using 3D printed polymer-zeolite composites. *ACS ES&T Water*, *1*(3), 621-629. http://doi.org/10.1021/acsestwater.0c00131.
12. Tengku Yasim-Anuar, T. A., Yee-Foong, L. N., Lawal, A. A., Farid, M. A. A., Yusuf, M. Z. M., Hassan, M. A., & Ariffin, H. (2022). Emerging application of biochar as a renewable and superior filler in polymer composites. *RSC Advances*, *12*(22), 13938-13949. http://doi.org/10.1039/D2RA01897G. PMid:35558839.
13. Zhong, Q., Shi, G., Sun, Q., Mu, P., & Li, J. (2021). Robust PVA-GO-TiO2 composite membrane for efficient separation oil-in-water emulsions with stable high flux. *Journal of Membrane Science*, *640*, 119836. http://doi.org/10.1016/j.memsci.2021.119836.
14. Zeng, T., Yu, Y., Li, Z., Zuo, J., Kuai, Z., Jin, Y., Wang, Y., Wu, A., & Peng, C. (2019). 3D MnO2 nanotubes@reduced graphene oxide hydrogel as reusable adsorbent for the removal of heavy metal ions. *Materials Chemistry and Physics*, *231*, 105-108. http://doi.org/10.1016/j.matchemphys.2019.04.019.
15. Vidales, M. J. M., Nieto-Márquez, A., Morcuende, D., Atanes, E., Blaya, F., Soriano, E., & Fernández-Martínez, F. (2019). 3D printed floating photocatalysts for wastewater treatment. *Catalysis Today*, *328*, 157-163. http://doi.org/10.1016/j.cattod.2019.01.074.
16. Wang, D., Zhi, T., Liu, L., Li, Y., Yan, W., Tang, Y., He, B., Hu, L., Jing, C., & Jiang, G. (2022). 3D printing of TiO2 nano particles containing macrostructures for As(III) removal in water. *The Science of the Total Environment*, *815*, 152754. http://doi.org/10.1016/j.scitotenv.2021.152754. PMid:34995588.
17. Yang, Z.-F., Li, L.-Y., Hsieh, C.-T., Juang, R.-S., & Gandomi, Y. A. (2018). Fabrication of magnetic iron Oxide@Graphene composites for adsorption of copper ions from aqueous solutions. *Materials Chemistry and Physics*, *219*, 30-39. http://doi.org/10.1016/j.matchemphys.2018.07.053.
18. Thomas, C. M., Kumar, D., Scheel, R. A., Ramarao, B., & Nomura, C. T. (2022). Production of medium chain length polyhydroxyalkanoate copolymers from agro-industrial waste streams. *Biocatalysis and Agricultural Biotechnology*, *43*, 102385. http://doi.org/10.1016/j.bcab.2022.102385.
19. Baig, U., Al-Kuhaili, M. F., & Dastageer, M. A. (2023). Photo-responsive Zinc Oxide-coated alumina ceramic membrane with super-wettable and self-cleaning features fabricated by single step RF magnetron sputtering for oily water treatment. *Process Safety and Environmental Protection*, *175*, 541-553. http://doi.org/10.1016/j.psep.2023.05.044.

20. Zhao, X., Zhang, R., Liu, Y., He, M., Su, Y., Gao, C., & Jiang, Z. (2018). Antifouling membrane surface construction: chemistry plays a critical role. *Journal of Membrane Science*, *551*, 145-171. http://doi.org/10.1016/j.memsci.2018.01.039.
21. al-Shaeli, M., Al-Juboori, R. A., Al Aani, S., Ladewig, B. P., & Hilal, N. (2022). Natural and recycled materials for sustainable membrane modification: recent trends and prospects. *The Science of the Total Environment*, *838*(Pt 1), 156014. http://doi.org/10.1016/j.scitotenv.2022.156014. PMid:35584751.
22. Li, S., Huang, L., Wang, D., Zhou, S., Sun, X., Zhao, R., Wang, G., Yao, T., Zhao, K., & Chen, R. (2023). A review of 3D superhydrophilic porous materials for oil/water separation. *Separation and Purification Technology*, *326*, 124847. http://doi.org/10.1016/j.seppur.2023.124847.
23. Bashari, A., Koohestani, A. H. S., & Salamatipour, N. (2020). Eco-friendly Dual-functional textiles: green water-repellent & anti-bacterial. *Fibers and Polymers*, *21*(2), 317-323. http://doi.org/10.1007/s12221-020-9568-6.
24. AbdulKadir, W. A. F. W., Ahmad, A. L., & Boon Seng, O. (2021). Carnauba wax/halloysite nanotube with improved anti-wetting and permeability of hydrophobic PVDF membrane via DCMD. *Membranes (Basel)*, *11*(3), 228. http://doi.org/10.3390/membranes11030228. PMid:33807017.
25. Ali, A., Jamil, M. I., Jiang, J., Shoaib, M., Amin, B. U., Luo, S., Zhan, X., Chen, F., & Zhang, Q. (2020). An overview of controlled-biocide-release coating based on polymer resin for marine antifouling applications. *Journal of Polymer Research*, *27*(4), 85. http://doi.org/10.1007/s10965-020-02054-z.
26. Facchi, D. P., Facchi, S. P., Souza, P. R., Bonafé, E. G., Popat, K. C., Kipper, M. J., & Martins, A. F. (2022). Composite filter with antimicrobial and anti-adhesive properties based on electrospun poly(butylene adipate-co-terephthalate)/poly(acid lactic)/Tween 20 fibers associated with silver nanoparticles. *Journal of Membrane Science*, *650*, 120426. http://doi.org/10.1016/j.memsci.2022.120426.
27. Yang, J., Li, W., Mu, B., Xu, H., Hou, X., & Yang, Y. (2022). Simultaneous toughness and stiffness of 3D printed nano-reinforced polylactide matrix with complete stereo-complexation via hierarchical crystallinity and reactivity. *International Journal of Biological Macromolecules*, *202*, 482-493. http://doi.org/10.1016/j.ijbiomac.2022.01.090. PMid:35051500.
28. Hao, Y., Chu, Y., Zhang, M., Shi, W., Chen, Y., Li, D., & Li, L. (2022). Preparation of functional degradable antibacterial film and application in fresh-keeping of grass carp. *Journal of Agriculture and Food Research*, *9*, 100341. http://doi.org/10.1016/j.jafr.2022.100341.
29. Mathew, J., Das, J. P., Tp, M., & Kumar, S. (2022). Development of poly (butylene adipate-co-terephthalate) PBAT toughened poly (lactic acid) blends 3D printing filament. *Journal of Polymer Research*, *29*(11), 474. http://doi.org/10.1007/s10965-022-03320-y.
30. Shankar, S., & Rhim, J.-W. (2022). Effect of types of zinc oxide nanoparticles on structural, mechanical and antibacterial properties of poly(lactide)/poly(butylene adipate-co-terephthalate) composite films. *Food Packaging and Shelf Life*, *21*, 100327. http://doi.org/10.1016/j.fpsl.2019.100327.
31. Pascoalino, L. A., Souza, R. L., Marques, N. N., & Curti, P. S. (2020). Caracterização e avaliação do comportamento termorresponsivo de fibras de Ecovio®/ PNIPAAm eletrofiadas. *Matéria (Rio de Janeiro)*, *25*(3), e-12830. http://doi.org/10.1590/s1517-707620200003.1130.
32. Malinowski, R., Moraczewski, K., & Raszkowska-Kaczor, A. (2020). Studies on the uncrosslinked fraction of PLA/PBAT blends modified by electron radiation. *Materials (Basel)*, *13*(5), 1068. http://doi.org/10.3390/ma13051068. PMid:32121084.
33. Jamnongkan, T., Jaroensuk, O., Khankhuean, A., Laobuthee, A., Srisawat, N., Pangon, A., Mongkholrattanasit, R., Phuengphai, P., Wattanakornsiri, A., & Huang, C.-F. (2022). A comprehensive evaluation of mechanical, thermal, and antibacterial properties of PLA/ZnO nanoflower biocomposite filaments for 3D printing application. *Polymers*, *14*(3), 600. http://doi.org/10.3390/polym14030600. PMid:35160589.
34. Valerio, T. L., Maia, G. A. R., Gonçalves, L. F., Viomar, A., Banczek, E. P., & Rodrigues, P. R. P. (2019). Study of the Nb_2O_5 insertion in ZnO to dye-sensitized solar cells. *Materials Research*, *22*(suppl 1), e20180864. http://doi.org/10.1590/1980-5373-mr-2018-0864.
35. Anžlovar, A., Kržan, A., & Žagar, E. (2018). Degradation of PLA/ZnO and PHBV/ZnO composites prepared by melt processing. *Arabian Journal of Chemistry*, *11*(3), 343-352. http://doi.org/10.1016/j.arabjc.2017.07.001.
36. Ge, C., Xu, X., Ma, F., Zhou, J., & Du, C. (2022). Biomimetic modification of water-borne polymer coating with carnauba wax for controlled release of urea. *International Journal of Molecular Sciences*, *23*(13), 7422. http://doi.org/10.3390/ijms23137422.
37. Park, K., Sadeghi, K., Panda, P. K., Seo, J., & Seo, J. (2022). Ethylene vinyl acetate/low-density polyethylene/oyster shell powder composite films: Preparation, characterization, and antimicrobial properties for biomedical applications. *Journal of the Taiwan Institute of Chemical Engineers*, *134*, 104301. http://doi.org/10.1016/j.jtice.2022.104301.
38. Yan, D., Wang, Z., Guo, Z., Ma, Y., Wang, C., Tan, H., & Zhang, Y. (2020). Study on the properties of PLA/PBAT composite modified by nanohydroxyapatite. *Journal of Materials Research and Technology*, *9*(5), 11895-11904. http://doi.org/10.1016/j.jmrt.2020.08.062.
39. Thiyagu, T. T., Gokilakrishnan, G., Uvaraja, V. C., Maridurai, T., & Arun Prakash, V. R. (2022). Effect of SiO2/TiO2 and ZnO Nanoparticle on Cardanol Oil Compatibilized PLA/PBAT Biocomposite Packaging Film. *Silicon*, *14*(7), 3795-3808. http://doi.org/10.1007/s12633-021-01577-4.
40. Laput, O., Vasenina, I., Salvadori, M. C., Savkin, K., Zuza, D., & Kurzina, I. (2019). Low-temperature plasma treatment of polylactic acid and PLA/HA composite material. *Journal of Materials Science*, *54*(17), 11726-11738. http://doi.org/10.1007/s10853-019-03693-4.
41. Cao, M., Cui, T., Yue, Y., Li, C., Guo, X., Jia, X., & Wang, B. (2023). Preparation and Characterization for the Thermal Stability and Mechanical Property of PLA and PLA/CF Samples Built by FFF Approach. *Materials (Basel)*, *16*(14), 5023. http://doi.org/10.3390/ma16145023. PMid:37512297.
42. Benabid, F. Z., Kharchi, N., Zouai, F., Mourad, A.-H. I., & Benachour, D. (2019). Impact of co-mixing technique and surface modification of ZnO nanoparticles using stearic acid on their dispersion into HDPE to produce HDPE/ZnO nanocomposites. *Polymers & Polymer Composites*, *27*(7), 389-399. http://doi.org/10.1177/0967391119847353.
43. Li, Y., Sun, H., Zhang, Y., Xu, M., & Shi, S. Q. (2019). The three-dimensional heterostructure synthesis of ZnO/cellulosic fibers and its application for rubber composites. *Composites Science and Technology*, *177*, 10-17. http://doi.org/10.1016/j.compscitech.2019.04.012.
44. Aida, M. S., Alonizan, N. H., Hussein, M. A., Hjiri, M., Abdelaziz, O., Attaf, R., & Zarrad, B. (2022). Facile synthesis and antibacterial activity of bioplastic membrane containing in doped ZnO/cellulose acetate nanocomposite. *Journal of Inorganic and Organometallic Polymers and Materials*, *32*(4), 1223-1233. http://doi.org/10.1007/s10904-021-02171-2.
45. Barakat, M. A.Y., & El-Wakil, A. E.-A. (2021). Preparation and characterization of EVA/ZnO composites as piezoelectric

elements for ultrasonic transducers. *Materials Research Express*, *8*(10), 105304. http://doi.org/10.1088/2053-1591/ac29fb.

46. Liu, S., Li, L., Li, B., Zhu, J., & Li, X. (2022). Size effect of carnauba wax nanoparticles on water vapor and oxygen barrier properties of starch-based film. *Carbohydrate Polymers*, *296*, 119935. http://doi.org/10.1016/j.carbpol.2022.119935. PMid:36088025.
47. Magno, J. A. P., Da, S., Neto, V. P., Cavalcante, C. E. C., Queiroz, S. K. S. S., Queiroz, I. S., Jr., Fraga, F. E. N., Andrade, H. D., & Melo, R. R. (2021). Synthesis and characterization of organic substrate in the S band for application in microstrip antennas. *Journal of Materials Science Materials in Electronics*, *32*(2), 1829-1841. http://doi.org/10.1007/s10854-020-04951-x.
48. Milanovic, J., Levic, S., Manojlovic, V., Nedovic, V., & Bugarski, B. (2011). Carnauba wax microparticles produced by melt dispersion technique. *Chemical Papers*, *65*(2), 213-220. http://doi.org/10.2478/s11696-011-0001-x.
49. Villalobos-Hernández, J. R., & Müller-Goymann, C. C. (2006). Sun protection enhancement of titanium dioxide crystals by the use of carnauba wax nanoparticles: the synergistic interaction between organic and inorganic sunscreens at nanoscale. *International Journal of Pharmaceutics*, *322*(1-2), 161-170. http://doi.org/10.1016/j.ijpharm.2006.05.037. PMid:16824709.
50. Ning, X., Song, X., Zhang, S., Wang, Y., & Feng, Y. (2022). Insights into flow improving for waxy crude oil doped with EVA/SiO2 nanohybrids. *ACS Omega*, *7*(7), 5853-5863. http://doi.org/10.1021/acsomega.1c05953. PMid:35224346.
51. Jian, W., Jin, Z., Yang, J., Meng, G., Liu, H., & Liu, H. (2022). Anticorrosion and antibiofouling performance of in-situ prepared layered double hydroxide coating modified by sodium pyrithione on aluminum alloy 7075. *Journal of Industrial and Engineering Chemistry*, *113*, 419-430. http://doi.org/10.1016/j.jiec.2022.06.017.
52. Rebelo, R. C., Gonçalves, L. P. C., Fonseca, A. C., Fonseca, J., Rola, M., Coelho, J. F. J., Rola, F., & Serra, A. C. (2022). Increased degradation of PLA/PBAT blends with organic acids and derivatives in outdoor weathering and marine environment. *Polymer*, *256*, 125223. http://doi.org/10.1016/j.polymer.2022.125223.
53. Çoban, O., Bora, M. Ö., Kutluk, T., & Özkoç, G. (2018). Mechanical and thermal properties of volcanic particle filled PLA/PBAT composites. *Polymer Composites*, *39*(S3), E1500-E1511. http://doi.org/10.1002/pc.24393.
54. Ding, Y., Zhang, C., Luo, C., Chen, Y., Zhou, Y., Yao, B., Dong, L., Du, X., & Ji, J. (2021). Effect of talc and diatomite on compatible, morphological, and mechanical behavior of PLA/PBAT blends. *E-Polymers*, *21*(1), 234-243. http://doi.org/10.1515/epoly-2021-0022.
55. Pietrosanto, A., Scarfato, P., Di Maio, L., Nobile, M. R., & Incarnato, L. (2020). Evaluation of the suitability of poly(lactide)/poly(butylene-adipate-co-terephthalate) blown films for chilled and frozen food packaging applications. *Polymers*, *12*(4), 804. http://doi.org/10.3390/polym12040804. PMid:32260170.
56. Prasong, W., Muanchan, P., Ishigami, A., Thumsorn, S., Kurose, T., & Ito, H. (2020). Properties of 3D printable poly(lactic acid)/poly(butylene adipate-co-terephthalate) blends and nano talc composites. *Journal of Nanomaterials*, *8040517*, 1-16. http://doi.org/10.1155/2020/8040517.
57. Pascual-González, C., de la Vega, J., Thompson, C., Fernández-Blázquez, J. P., Herráez-Molinero, D., Biurrun, N., Lizarralde, I., Sánchez del Río, J., & González, C. (2022). Processing and mechanical properties of novel biodegradable poly-lactic acid/Zn 3D printed scaffolds for application in tissue regeneration. *Journal of the Mechanical Behavior of Biomedical Materials*, *132*, 105290. http://doi.org/10.1016/j.jmbbm.2022.105290. PMid:35671668.
58. Spoerk, M., Sapkota, J., Weingrill, G., Fischinger, T., Arbeiter, F., & Holzer, C. (2017). Shrinkage and warpage optimization of expanded-perlite-filled polypropylene composites in extrusion-based additive manufacturing. *Macromolecular Materials and Engineering*, *302*(10), 1700143. http://doi.org/10.1002/mame.201700143.
59. Kodali, D., Umerah, C. O., Idrees, M. O., Jeelani, S., & Rangari, V. K. (2021). Fabrication and characterization of polycarbonate-silica filaments for 3D printing applications. *Journal of Composite Materials*, *55*(30), 4575-4584. http://doi.org/10.1177/00219983211044748.

Received: Mar. 23, 2024
Revised: June 01, 2024
Accepted: June 06, 2024